DALTON
FULL PAPER

Nickel–iron–sulfur complexes: approaching structural analogues of the active sites of NiFe-hydrogenase and carbon monoxide dehydrogenase/acetyl-CoA synthase

Matt C. Smith,[a] J. Elaine Barclay,[a] Stephen P. Cramer,[b] Sian C. Davies,[a] Wei-Wei Gu,[b] David L. Hughes,[a] Steven Longhurst[a] and David J. Evans *[a]

[a] *Department of Biological Chemistry, John Innes Centre, Norwich Research Park, Colney, UK NR4 7UH. E-mail: dave.evans@bbsrc.ac.uk*
[b] *Department of Applied Science, University of California Davis, CA 95616, USA*

Received 12th February 2002, Accepted 26th April 2002

The NiFe-dinuclear complexes [{Fe(NS$_3$)(CO)$_2$-S,S'}NiCl(dppe)] **1**, [{Fe(NS$_3$)(CO)-S,S'}NiCl(dppe)] **2**, [{Fe(NS$_3$)(NO)-S,S'}NiCl(dppe)] **3**, [{Fe(NS$_3$)(NO)-S,S'}Ni(CH$_3$)(dppe)] **4**, [Ni{Fe(NS$_3$)(CO)-S,S'}$_2$] **5** have been prepared using the anions [Fe(NS$_3$)(CO)]$^-$ and [Fe(NS$_3$)(NO)]$^-$ (NS$_3$ = N(CH$_2$CH$_2$S)$_3{}^{3-}$) as chelate ligands to nickel. Crystal structure characterisation has been carried out on **1**, **3** and **5**. The spectroscopic properties of the complexes have been measured. Complex **1** is a good structural analogue of the active form of the active site of NiFe-hydrogenase. Complexes **1**–**5** also show features related to the active sites of the nickel enzymes carbon monoxide dehydrogenase and acetyl-CoA synthase.

Introduction

The nickel containing enzymes NiFe-hydrogenase and carbon monoxide dehydrogenase/acetyl-CoA synthase (CODH/ACS) are of major environmental and potential industrial importance. Hydrogenases catalyse the reversible reduction of protons to dihydrogen. CODH/ACS catalyse the reversible interconversion of carbon dioxide and carbon monoxide and catalyse formation or catabolism of acetyl-CoA.

The NiFe-hydrogenase from *Desulfovibrio gigas*, as aerobically isolated in the inactive form, has been characterised by X-ray crystallography.[1,2] This indicates that the active site is most likely a dinuclear thiolate-bridged nickel–iron complex in which the nickel atom is coordinated by four cysteinate-sulfur atoms, two of which bridge to the iron atom. In the aerobically isolated crystals there is an additional bridging feature, probably oxo or hydroxo, which is unlikely to be present in the active form of the enzyme.[2,3] The other ligands to iron, as shown by crystallography and spectroscopy,[2,4] are, unusually for biology, two cyanides and one carbon monoxide.

The recently published[5] crystal structure, at 1.6 Å resolution, of the dithionite-reduced state of CODH from *Carboxydothermus hydrogenoformans* shows the active centre, Cluster C, to be a unique asymmetric {NiFe$_4$S$_5$} assembly, Fig. 1a. The nickel is four-coordinate square planar and one of the iron atoms is extraneous to the cuboidal-like core. This iron atom is bound through two bridging-sulfides to a nickel atom and two iron atoms of the {NiFe$_3$S$_3$} core. Other ligands to the extraneous iron are a cysteinate-sulfur and a histidine-nitrogen. The crystal structure,[6] at 2.8 Å resolution, of CODH from *Rhodospirillum rubrum* preincubated with carbon monoxide shows Cluster C to have a similar structure except: the cuboidal fragment is "closed"; the extraneous iron atom is connected to the cluster through a shared sulfide and a bridging cysteinate-sulfur; the nickel is five-coordinate, the fifth ligand being, possibly, non-substrate carbon monoxide, Fig. 1b. Previously it had been proposed that the Cluster C of CODH from *R. rubrum* contains a binuclear FeNi-fragment linked, probably, through cysteinate-sulfur to an {Fe$_4$S$_4$} cluster.[7]

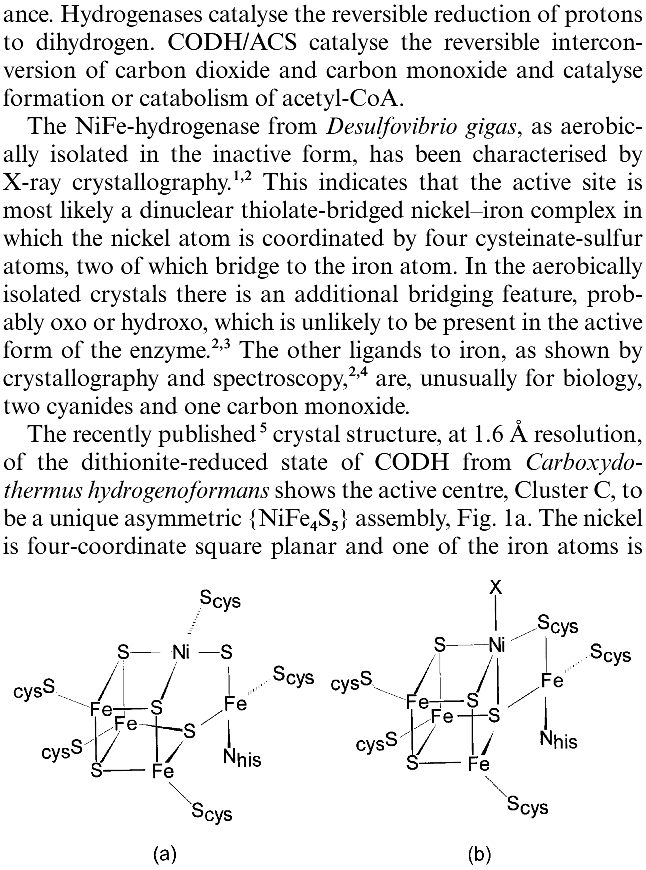

(a) (b)

Fig. 1 A representation of the active site assembly of (a) reduced CODH from *C. hydrogenoformans* and (b) of CO-preincubated CODH from *R. rubrum*, X is an unidentified ligand, possibly non-substrate CO.

There is no reported high resolution crystal structure of a bifunctional CODH/ACS protein. It is expected that CODH Cluster C from a bifunctional CODH/ACS protein will have the same structure as that described above. However, extensive biochemical and spectroscopic studies support the suggestion that the active centre of the ACS unit, Cluster A, has a nickel atom, in square planar geometry, bridged, probably through sulfur, to a "classic" {Fe$_4$S$_4$} cluster.[8] The mechanism of the ACS reaction apparently involves metal–carbonyl, methyl–metal and acyl–metal intermediates.[8]

Here we have employed the anions [Fe(NS$_3$)(CO)]$^-$ and [Fe(NS$_3$)(NO)]$^-$ (NS$_3$ = N(CH$_2$CH$_2$S)$_3{}^{3-}$)[9,10] as chelate ligands to nickel to prepare nickel–iron complexes which have structural features with similarities to the active site of NiFe-hydrogenase and some features similar to those of the active sites of CODH/ACS. Some of this work has been published in preliminary form[11,12] and other work in this and related areas recently reviewed.[13]

Results and discussion

Synthesis

The reaction, under a CO atmosphere, of [NiCl$_2$(dppe)] with [NEt$_4$][Fe(NS$_3$)(CO)] gave the dinuclear complex [{Fe(NS$_3$)-

DOI: 10.1039/b201578c

(CO)$_2$-*S*,*S*′}NiCl(dppe)] **1** in good yield. When the synthesis was performed under dinitrogen or argon, rather than CO, the monocarbonyl complex [{Fe(*N*S$_3$)(CO)-*S*,*S*′}NiCl(dppe)] **2** was formed. Complex **2** was never obtained analytically pure (it could not be separated from a small amount of dicarbonyl-complex contaminant) nor could we obtain crystals. When an acetonitrile solution of **2** was stirred under a CO atmosphere it was converted, quantitatively, back to the dicarbonyl-complex **1**. Attempts to exchange CO by cyanide in **1** or to introduce cyanide at iron in **2** were unsuccessful, although CO exchange was facile (see below). Use of the iron–nitrosyl chelate, [Fe(*N*S$_3$)(NO)]$^-$, in a reaction similar to that used to prepare complex **2** gave, in good yield, the nitrosyl complex [{Fe(*N*S$_3$)(NO)-*S*,*S*′}NiCl(dppe)] **3**. When complex **3** was prepared under a CO atmosphere, no carbonyl was bound to the iron atom. The iron–nitrosyl chelate reacted with [NiCl(CH$_3$)(dppe)] to give the methylated-nickel dinuclear complex [{Fe(*N*S$_3$)(NO)-*S*,*S*′}Ni(CH$_3$)(dppe)] **4**. Reaction of the iron–carbonyl chelate with [NiCl(CH$_3$)(dppe)] did not give a methylated-nickel dinuclear complex nor did reaction of the iron–nitrosyl chelate with [Ni(CH$_3$)$_2$(dppe)]. Complex **4** can be considered to be an analogue of a proposed[8] nickel–methyl intermediate in the catalytic cycle of ACS, Fig. 2, and is the first example of a methylated-nickel in a dinuclear NiFe complex. The reaction of the dmso solvate of nickel(II) chloride with two equivalents of [NEt$_4$][Fe(*N*S$_3$)(CO)] gave the linear trinuclear complex [Ni{Fe(*N*S$_3$)(CO)-*S*,*S*′}$_2$] **5**. Complexes **1**–**5**, in the solid state, are moderately stable to air but they are more sensitive in solution.

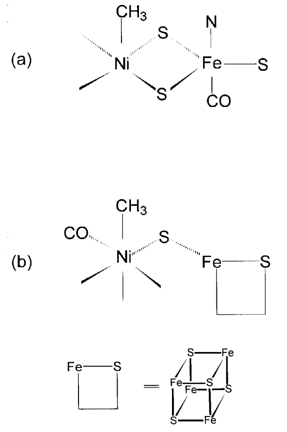

Fig. 2 A schematic comparison of (a) the core of complex **4** and (b) the proposed nickel–methyl intermediate in the ACS mechanism.

Structures

[{Fe(*N*S$_3$)(CO)$_2$-*S*,*S*′}NiCl(dppe)], 1. The structure of dinuclear complex **1** is shown in Fig. 3 and selected bond lengths and angles are listed in Table 1. The iron atom is octahedrally coordinated, with two of the thiolate ligand arms also bridging to the nickel atom. The nickel is five-coordinate in a square pyramidal pattern in which the nickel atom is displaced 0.307(2)Å from the base plane towards the chloride ligand in the apical site. The normals to the S$_3$C 'equatorial' plane about the iron atom and the P$_2$S$_2$ base plane about the nickel atom are inclined at 19.4(1)°. The *N*S$_3$ ligand arrangement is different from those reported previously[9,14] in trigonal bipyramidal complexes of iron and vanadium, where there is approximate three-fold symmetry in the ligand. Here, the three thiolate sulfur atoms are arranged meridionally about the iron and the pair of mutually *trans* thiolate arms of the ligand are essentially mirror images (with opposite S–C–C–N torsion angles). The carbonyl ligands are opposite the amino nitrogen atom and one of the bridging sulfur atoms.

Table 1 Selected molecular dimensions (bond lengths in Å, angles and torsion angles in °) in complex **1**

Fe ··· Ni	3.308(2)	Ni–Cl	2.508(3)
Fe–S(1)	2.281(3)	Ni–S(1)	2.247(3)
Fe–S(2)	2.331(3)	Ni–S(2)	2.255(3)
Fe–S(3)	2.306(3)	Ni–P(1)	2.164(3)
Fe–N(4)	2.031(8)	Ni–P(2)	2.196(3)
Fe–C(5)	1.783(12)	C(5)–O(5)	1.137(11)
Fe–C(6)	1.741(10)	C(6)–O(6)	1.150(10)
S(2)–Fe–S(1)	85.18(9)	S(2)–Ni–S(1)	87.78(9)
S(3)–Fe–S(1)	172.57(12)	P(1)–Ni–S(1)	87.77(10)
N(4)–Fe–S(1)	86.3(2)	P(2)–Ni–S(1)	160.26(11)
C(5)–Fe–S(1)	95.3(3)	S(1)–Ni–Cl	107.27(9)
C(6)–Fe–S(1)	91.8(3)	P(1)–Ni–S(2)	167.30(11)
S(3)–Fe–S(2)	92.89(11)	P(2)–Ni–S(2)	93.51(10)
N(4)–Fe–S(2)	87.6(2)	S(2)–Ni–Cl	103.38(10)
C(5)–Fe–S(2)	177.9(4)	P(1)–Ni–P(2)	86.73(10)
C(6)–Fe–S(2)	85.8(3)	P(1)–Ni–Cl	89.29(9)
N(4)–Fe–S(3)	86.5(2)	P(2)–Ni–Cl	91.62(9)
C(5)–Fe–S(3)	86.8(3)	Ni–S(1)–Fe	93.86(10)
C(6)–Fe–S(3)	95.2(3)	C(14)–S(1)–Ni	107.9(4)
C(5)–Fe–N(4)	94.4(4)	C(14)–S(1)–Fe	99.6(3)
C(6)–Fe–N(4)	173.3(4)	Ni–S(2)–Fe	92.31(10)
C(6)–Fe–C(5)	92.2(5)	C(24)–S(2)–Ni	109.4(3)
O(5)–C(5)–Fe	177.6(10)	C(24)–S(2)–Fe	96.3(3)
O(6)–C(6)–Fe	174.7(9)	C(34)–S(3)–Fe	97.9(3)
S(1)–C(14)–C(41)–N(4)	40.9(10)		
S(2)–C(24)–C(42)–N(4)	46.2(9)		
S(3)–C(34)–C(43)–N(4)	−50.3(10)		
P(1)–C(12)–C(21)–P(2)	−44.9(7)		

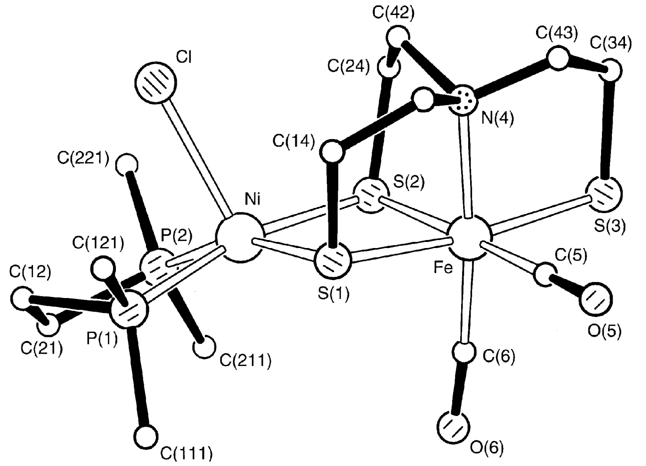

Fig. 3 A molecule of [{Fe(*N*S$_3$)(CO)$_2$-*S*,*S*′}NiCl(dppe)] **1** showing the principal atoms. The phenyl groups of the dppe ligand and all the hydrogen atoms have been omitted for clarity.

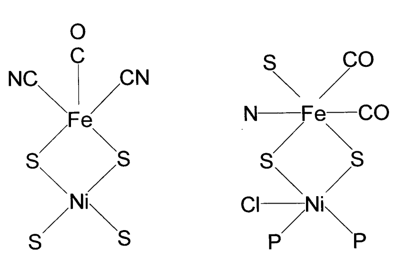

Fig. 4 A schematic comparison of the proposed NiFe-hydrogenase active site (left) and the core of complex **1** (right).

Complex **1** is a good structural analogue of the proposed active site of NiFe-hydrogenase, Fig 4. The core of **1** is dinuclear with nickel bound to iron by a bis(thiolate-bridge) and the iron atom binds two carbon monoxides. The Ni ··· Fe distance of 3.308(2) Å is similar to that found for other thiolate-bridged nickel complexes (2.80–3.76 Å[15–19]) but is longer than the Ni ··· Fe distance, 2.9 Å, in the as isolated, inactive NiFe-

Table 2 Selected molecular dimensions (bond lengths in Å, angles and torsion angles in °) in complex **3**

Fe ··· Ni	3.0216(5)		
Fe–S(1)	2.3405(8)	Ni–S(1)	2.3065(7)
Fe–S(2)	2.3397(8)	Ni–S(2)	2.3577(7)
Fe–S(3)	2.2579(9)	Ni–P(1)	2.1892(7)
Fe–N(4)	2.265(2)	Ni–P(2)	2.1750(7)
Fe–N(5)	1.728(3)	Ni–Cl	2.4334(8)
N(5)–O(5a)	1.289(10)	N(5)–O(5c)	1.236(11)
N(5)–O(5b)	1.291(10)	N(5)–O(5d)	1.151(12)
S(2)–Fe–S(1)	96.78(3)	S(2)–Ni–S(1)	97.22(3)
S(3)–Fe–S(1)	126.77(3)	P(1)–Ni–S(1)	86.54(3)
N(4)–Fe–S(1)	83.54(6)	P(2)–Ni–S(1)	169.98(3)
N(5)–Fe–S(1)	100.61(10)	S(1)–Ni–Cl	99.43(3)
S(3)–Fe–S(2)	132.69(3)	P(1)–Ni–S(2)	147.97(3)
N(4)–Fe–S(2)	82.73(6)	P(2)–Ni–S(2)	85.78(3)
N(5)–Fe–S(2)	99.97(10)	S(2)–Ni–Cl	103.49(3)
S(3)–Fe–N(4)	84.69(6)	P(2)–Ni–P(1)	85.91(3)
N(5)–Fe–S(3)	90.13(10)	P(1)–Ni–Cl	107.25(3)
N(5)–Fe–N(4)	174.67(11)	P(2)–Ni–Cl	89.10(3)
Ni–S(1)–Fe	81.11(3)	C(34)–S(3)–Fe	102.11(11)
C(14)–S(1)–Ni	109.24(10)	O(5a)–N(5)–Fe	138.4(6)
C(14)–S(1)–Fe	100.50(9)	O(5b)–N(5)–Fe	141.4(6)
Fe–S(2)–Ni	80.07(3)	O(5c)–N(5)–Fe	142.0(6)
C(24)–S(2)–Ni	111.11(10)	O(5d)–N(5)–Fe	169.8(7)
C(24)–S(2)–Fe	101.48(9)		
S(1)–C(14)–C(41)–N(4)	−48.0(5)		
S(2)–C(24)–C(42)–N(4)	−49.9(4)		
S(3)–C(34)–C(43)–N(4)	−39.7(6)		
S(1)–C(14)–C(41b)–N(4)	48.2(4)		
S(2)–C(24)–C(42b)–N(4)	49.4(4)		
S(3)–C(34)–C(43b)–N(4)	43.0(6)		
P(1)–C(12)–C(21)–P(2)	−49.4(2)		

hydrogenase.[1,2] However, theoretical calculations predict that in the active states of the enzyme the Ni ··· Fe distance is longer than 2.9 Å. For example, it has been calculated[20] that the Ni ··· Fe distance in the Ni–SI$_{1934}$ and Ni–SI$_{1914}$ states, the states at which the enzyme begins the catalytic cycle, are 3.24 and 3.13 Å respectively, more similar to that found for complex **1**. To temper this, X-ray absorption spectroscopic studies on *Chromatium vinosum* hydrogenase indicate a shortening of the Ni ··· Fe distance to 2.5–2.6 Å on reductive activation.[21]

[{Fe(*N*S$_3$)(NO)-*S*,*S*′}NiCl(dppe)]·MeCN, 3·MeCN. The structure of this complex is shown in Fig. 5 and selected bond lengths and angles are listed in Table 2. The iron atom is trigonal bipyramidally coordinated with the nitrosyl ligand in an axial position. The iron lies 0.2514(4) Å from the equatorial plane toward the nitrosyl ligand. Similar to complex **1** two of the thiolate ligand arms also are bridging to the nickel atom. The nickel has a coordination pattern which might be described as midway between square pyramidal (with Cl as the apical ligand) and trigonal bipyramidal (with S(1) and P(2) as the axial groups). There is disorder in the nitrosyl ligand, with four distinct positions for the oxygen atoms. None of the positions form a linear O–N–Fe arrangement; three of the angles average to 140.6(11)° (N–O bond lengths average 1.27(2) Å) with the fourth being 169.8(7)° (N–O bond length 1.152(14) Å). The Ni ··· Fe distance, 3.0216(5) Å, is slightly shorter than that found in complex **1**.

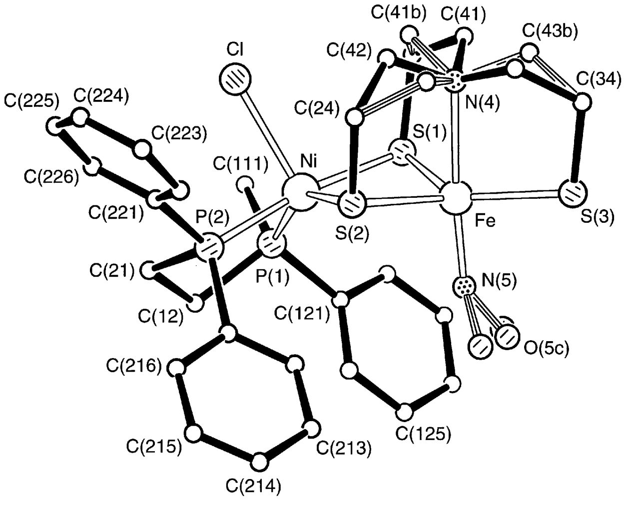

Fig. 5 A molecule of [{Fe(*N*S$_3$)(NO)-*S*,*S*′}NiCl(dppe)] **3** showing the disorder in the *N*S$_3$ and nitrosyl ligands; four distinct sites were identified for the nitrosyl O atom. One of the phenyl groups of the dppe ligand has been omitted for clarity.

Table 3 Selected molecular dimensions (bond lengths in Å, angles and torsion angles in °) in complex **5**

Fe ··· Ni	2.6372(11)	Fe–C(5)	1.780(10)
Fe–S(1)	2.266(2)	Ni–S(1)	2.229(2)
Fe–S(2)	2.249(2)	Ni–S(2)	2.287(2)
Fe–S(3)	2.207(2)	C(5)–O(5a)	1.13(5)
Fe–N(4)	2.046(6)	C(5)–O(5b)	1.15(5)
S(2)–Fe–S(1)	107.26(8)	S(1)–Ni–S(1′)	124.20(14)
S(3)–Fe–S(1)	123.62(10)	S(1)–Ni–S(2)	107.19(8)
N(4)–Fe–S(1)	88.0(2)	S(1)–Ni–S(2′)	103.00(8)
C(5)–Fe–S(1)	95.7(4)	S(2)–Ni–S(2′)	112.42(14)
S(3)–Fe–S(2)	128.76(10)	Ni–S(1)–Fe	71.83(7)
N(4)–Fe–S(2)	87.5(2)	C(14)–S(1)–Ni	108.2(3)
C(5)–Fe–S(2)	94.0(4)	C(14)–S(1)–Fe	98.2(3)
N(4)–Fe–S(3)	88.6(2)	Fe–S(2)–Ni	71.10(7)
C(5)–Fe–S(3)	87.1(3)	O(5a)–C(5)–Fe	167(2)
C(5)–Fe–N(4)	175.4(3)	O(5b)–C(5)–Fe	170(3)
C(24)–S(2)–Ni	106.7(3)	C(34)–S(3)–Fe	99.7(3)
C(24)–S(2)–Fe	100.2(3)		
S(1)–C(14)–C(41)–N(4)	50.3(8)		
S(2)–C(24)–C(42)–N(4)	46.8(8)		
S(3)–C(34)–C(43)–N(4)	50.4(9)		

Symmetry transformation: ′ : $-x, 1 - y, z$.

[Ni{Fe(*N*S$_3$)(CO)-*S*,*S*′}$_2$], 5. This complex is made up of two trigonal bipyramidal Fe(*N*S$_3$)(CO) units, each of which bridges to a central nickel atom, which lies on a two-fold symmetry axis and is slightly distorted from regular tetrahedral geometry, Fig. 6. Selected bond lengths and angles are listed in Table 3.

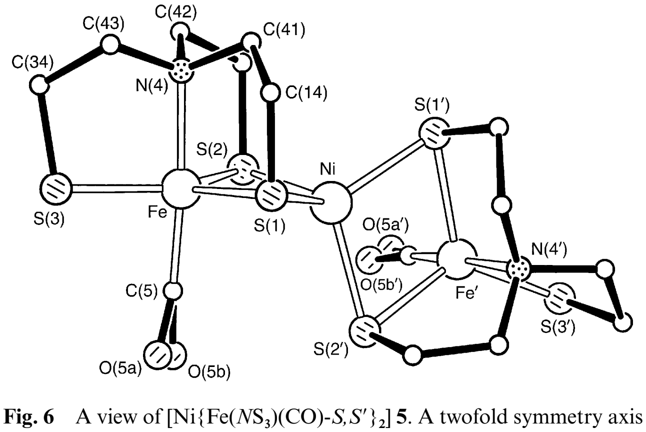

Fig. 6 A view of [Ni{Fe(*N*S$_3$)(CO)-*S*,*S*′}$_2$] **5**. A twofold symmetry axis through Ni relates the two Fe(*N*S$_3$)(CO) units. The carbonyl ligands are disordered, with two distinct sites for O(5).

Complex **5** is isostructural with the analogous complexes [Fe{Fe(*N*S$_3$)(CO)-*S*,*S*′}$_2$] **6** and [Co{Fe(*N*S$_3$)(CO)-*S*,*S*′}$_2$] **7**;[9] the iron and nickel complexes show alternative sites for the carbonyl O-atom, but no disorder was found in the cobalt complex. Only in the dimensions about the central metals of these complexes do we note any significant variation: in each complex, one pair of M–S distances is longer than the other; the longer distance at *ca* 2.29 Å is constant but the shorter distance decreases from 2.2775(2) Å in the iron complex **6** to 2.242(2) Å for cobalt **7** and 2.229(2) Å for nickel **5**. The crystallographic cell lengths show corresponding slight decreases. In complex **5**, the shorter Ni–S distance is marginally shorter than in most reported approximately tetrahedral Ni–S_4 complexes. In NiS_4 complexes with four terminal Ni–S bonds, such as $[Ni(SR)_4]^{2-}$ (R = aryl), there are two S–Ni–S angles of *ca* 90° involving opposite pairs of thiolate ligands,[22,23] in thiolate bis-bridged dinuclear complexes, *e.g.* $[Ni_2(S^tBu)_6]^{2-}$, there is one angle of *ca.* 84° (subtended by the bridging S atoms) and an opposite large angle of *ca.* 130° (between the terminal S atoms),[23] and in the only trinuclear, bis-bridged, Ni_3 complex, $[Ni_3(LS)_4]^{2+}$ (LSH = (2-sulfanylphenyl)bis(pyrazolyl)methane), the central, tetrahedral nickel has two opposing angles of *ca.* 90° (both in Ni_2S_2 rings).[24] Complex **5** has a more regular tetrahedral shape with S–Ni–S angles in the range 103.00(8) to 124.20(14)°. We also note that the $Ni \cdots Ni$ distances in the bridged complexes are all *ca.* 3.4 Å whereas the $Ni \cdots Fe$ distance in complex **5** is much shorter at 2.6372(11) Å.

Spectroscopy

X-Ray absorption spectroscopy. The XANES spectra, Fig. 7, of complexes **1** and **5** show their nickel environment to be quite different. Complex **1** shows a clear pre-edge feature at ≈8336 eV consistent with the square pyramidal geometry defined by crystallography. The tetrahedral geometry about nickel in complex **5** is supported by a pre-edge peak at ≈8331 eV; tetrahedral complexes have strong $1s \longrightarrow 3d$ transitions because p–d mixing is allowed in this geometry. There is no $1s \longrightarrow 4p_z$ peak at ≈8336 eV in the spectrum of **5**, thus ruling out a planar four-coordinate or pyramidal five-coordinate geometry. An EPR spectrum of a frozen dmf solution of **5** shows $S = 1$ ($g_\parallel = 4.0$) and is further confirmation that the nickel atom has tetrahedral coordination in this complex. Ni-EXAFS data for complex **1** (4 × S at 2.18 Å; 1 × Cl at 2.48 Å; 1 × Fe at 3.29 Å) and complex **5** (4 × S at 2.23 Å; 2 × Fe at 2.61 Å) are in good agreement with the crystallographically determined dimensions about the nickel atom.

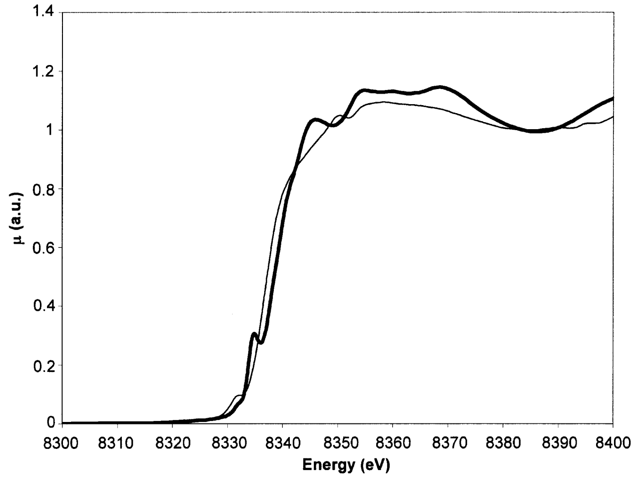

Fig. 7 The XANES spectra of $[\{Fe(\mathit{N}S_3)(CO)_2\text{-}\mathit{S,S'}\}NiCl(dppe)]$ **1** (bold line) and $[Ni\{Fe(\mathit{N}S_3)(CO)\text{-}\mathit{S,S'}\}_2]$ **5** (thin line).

Table 4 Infrared carbonyl stretching frequencies (cm^{-1}) for isotopically labelled $[\{Fe(\mathit{N}S_3)(^nCO)(^mCO)\text{-}\mathit{S,S'}\}NiCl(dppe)]$

		Solid[a]		Solution[b]	
$^nC^{16}O$	$^mC^{16}O$	Found	Calc.	Found	Calc.
12	12	2000	—	2013	—
		1944	—	1955	—
13	13	1952	1955	1967	1968
		1899	1899	1911	1911
12	13	1984	—	1998	—
		1916	—	1924	—
$13(^{18}O)$	$13(^{16}O)$	1940	—	1948	—
		1870	—	1882	—
$13(^{18}O)$	$13(^{18}O)$	1910	1903	n.o.[c]	1917
		1851	1851	n.o.	1863

[a] KBr disc. [b] Dichloromethane. [c] n.o. = not observed.

Infrared. The dicarbonyl complex **1** shows, in the solid state, two coupled infrared peaks at 1944 and 2000 cm^{-1}. Bubbling dinitrogen through a dichloromethane solution of dicarbonyl **1** results in a decrease of the infrared peaks arising from **1** {νCO (CH_2Cl_2) 2013 and 1955 cm^{-1}} and the growth of a peak at 1907 cm^{-1} consistent with formation of the monocarbonyl **2**. This conversion, under the conditions employed, is never complete. Passing carbon monoxide through the solution of the mixture formed, regenerates the dicarbonyl quantitatively. Isotopically labelled **1** can be prepared by reaction of $[NEt_4][Fe(\mathit{N}S_3)(^{13}CO)]$ with $[NiCl_2(dppe)]$ under an atmosphere of ^{13}CO. The value of the carbonyl stretches for $[\{Fe(\mathit{N}S_3)(^{13}CO)_2\text{-}\mathit{S,S'}\}NiCl(dppe)]$, in the solid and dichloromethane solution, are shown in Table 4. The isotopically shifted stretches are in good agreement with those calculated. The spectrum was further complicated by the presence of $^{13}C^{18}O$ in the isotopically enriched carbon monoxide; two additional peaks in the spectrum are assigned to the coupled carbonyl stretches of $[\{Fe(\mathit{N}S_3)(^{13}C^{16}O)(^{13}C^{18}O)\text{-}\mathit{S,S'}\}NiCl(dppe)]$. Peaks arising from $[\{Fe(\mathit{N}S_3)(^{13}C^{18}O)_2\text{-}\mathit{S,S'}\}NiCl(dppe)]$, calculated as 1903 and 1851 cm^{-1}, are not observed. Reaction of $[NiCl_2(dppe)]$ with $[NEt_4][Fe(\mathit{N}S_3)(^{12}CO)]$ under excess ^{13}CO gave a material with a spectrum consistent with a mixture of $[\{Fe(\mathit{N}S_3)(^{12}CO)(^{13}CO)\text{-}\mathit{S,S'}\}NiCl(dppe)]$, $[\{Fe(\mathit{N}S_3)(^{13}CO)_2\text{-}\mathit{S,S'}\}NiCl(dppe)]$, $[\{Fe(\mathit{N}S_3)(^{13}C^{16}O)(^{13}C^{18}O)\text{-}\mathit{S,S'}\}NiCl(dppe)]$ and, as a very minor component, $[\{Fe(\mathit{N}S_3)(^{13}C^{18}O)_2\text{-}\mathit{S,S'}\}NiCl(dppe)]$. The absence of any significant amount of $[\{Fe(\mathit{N}S_3)(^{12}CO)_2\text{-}\mathit{S,S'}\}NiCl(dppe)]$ is consistent with the reaction being performed under an excess of ^{13}CO. The converse reaction, $[NiCl_2(dppe)]$ with $[NEt_4][Fe(\mathit{N}S_3)(^{13}CO)]$ under ^{12}CO, gave a mixture of $[\{Fe(\mathit{N}S_3)(^{12}CO)_2\text{-}\mathit{S,S'}\}NiCl(dppe)]$, $[\{Fe(\mathit{N}S_3)(^{12}CO)(^{13}CO)\text{-}\mathit{S,S'}\}NiCl(dppe)]$ and, as a minor component, $[\{Fe(\mathit{N}S_3)(^{13}CO)_2\text{-}\mathit{S,S'}\}NiCl(dppe)]$. The values for the carbonyl stretches of $[\{Fe(\mathit{N}S_3)(^nCO)(^mCO)\text{-}\mathit{S,S'}\}NiCl(dppe)]$ are listed in Table 4. Under the experimental conditions, exchange and scrambling of the carbonyls has occurred. Carbon monoxide exchange in MeCN solution also has been demonstrated for the precursor complex $[NEt_4][Fe(\mathit{N}S_3)(CO)]$, eqn. (1), ($\nu^{12}CO$ = 1905 cm^{-1}; $\nu^{13}CO$ = 1860 cm^{-1}, calc. 1862 cm^{-1}).

$$[NEt_4][Fe(\mathit{N}S_3)(^{12}CO)] + {}^{13}CO \rightleftharpoons [NEt_4][Fe(\mathit{N}S_3)(^{13}CO)] + {}^{12}CO \quad (1)$$

The solid state infrared carbonyl stretch of trinuclear **5** at 1933 cm^{-1} is similar to that observed for the analogous iron **6** (1937 cm^{-1}) and cobalt **7** (1938 cm^{-1}) complexes.[9] The $^{13}C^{16/18}O$ labelled complexes have also been isolated and the values for their carbonyl stretching frequencies are listed, together with calculated values to which they show good agreement, in Table 5. There is no coupling, as expected, between the carbonyl groups on the terminal iron atoms.

The nitrosyl complexes **3** and **4** exhibit ν_{NO} at 1667 and 1666 cm^{-1}, respectively, these are in the same region as those found for a range of other $Fe(\mathit{N}S_3)$–nitrosyl complexes[10] and are consistent with the nitrosyl ligand being considered formally as NO^- (see below).

Mössbauer. The Mössbauer spectra of complexes **1**–**5** are symmetric quadrupole split doublets, *e.g.* Fig. 8; the derived

Table 5 Infrared carbonyl stretching frequencies (cm^{-1}) for [M{Fe(*N*S$_3$)(CO)-*S*,*S*′}$_2$] (M = Fe, Co, Ni) with isotopically-substituted carbonyl ligand. Calculated values in parentheses

	Fe	Co	Ni
^{12}C^{16}O	1937	1938	1933
^{13}C^{16}O	1890 (1894)	1890 (1894)	1888 (1891)
^{13}C^{18}O	1850 (1846)	1850 (1846)	1848 (1843)

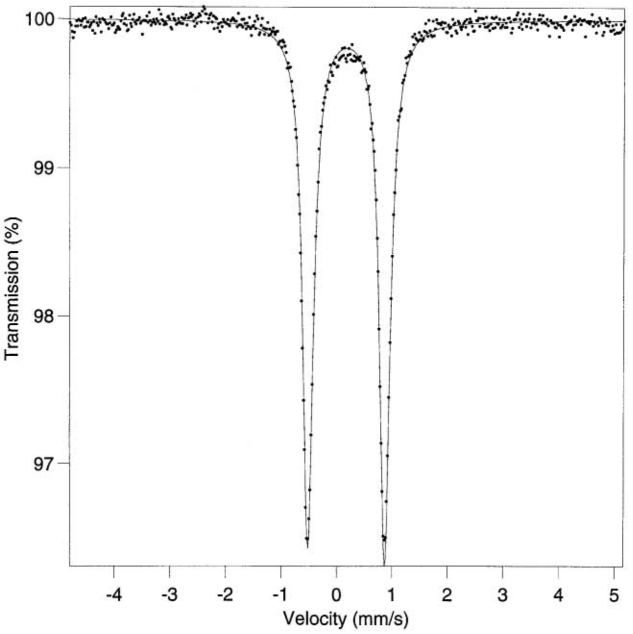

Fig. 8 The Mössbauer spectrum of [Ni{Fe(*N*S$_3$)(CO)-*S*,*S*′}$_2$] **5** at 77 K.

parameters for these and some related complexes are listed in Table 6. The values of isomer shift (i.s.) and quadrupole splitting (q.s.) for **1** and **2** are consistent with, respectively, octahedral and trigonal bipyramidal low-spin iron(II). The i.s. and temperature-independent (77–298 K) q.s. for the nitrosyl complexes **3** and **4**, together with the low nitrosyl infrared stretch for both complexes and the bent Fe–N–O arrangement in the structure of **3**, are consistent with a formal high-spin iron(III) oxidation state. The nitrosyl ligand is, therefore, considered to be present as NO$^-$ and enforces spin-pairing so that the spin-state of iron is S = 3/2. Complexes **3** and **4** are {FeNO}^{7} complexes in the Enemark and Feltham notation;[25] ground spin states of S = 3/2 have been found in several {FeNO}^{7} complexes and biological systems, featuring either five-coordinate (square pyramidal) or six-coordinate ligation. This S = 3/2 state has been described as arising from the high-spin ferric (S = 5/2) state being antiferromagnetically coupled to NO$^-$ (S = 1).[26] The observed parameters are similar to those reported for a series of {FeNO}^{7} trinuclear complexes, [M{Fe(*N*S$_3$)(NO)-*S*,*S*′}$_2$] (M = Fe, Co, Ni, Cu), containing the trigonal bipyramidal {Fe(*N*S$_3$)(NO)} moiety.[10] The complex **5** has an i.s. very similar to that of the related trinuclear complexes [M{Fe(*N*S$_3$)(CO)-S,S′}$_2$] (M = Fe **6**, Co **7**) consistent with iron(II). A gradual increase in q.s. with atomic number of the central metal atom is observed.

Conclusion

The metrical parameters for complex **1** make it a good structural analogue of the Ni–SI$_{1914/1934}$ states of the active site of NiFe-hydrogenase. We are now attempting to improve this analogy. The methylated-nickel complex **4** is the first example of a methylated-nickel in a di-heterometallic assembly and as such can be considered as having similarities to the methylated-nickel stage of the proposed mechanism for the action of ACS.

Table 6 Mössbauer parameters at 77 K in zero field[a]

Complex	i.s.	q.s.
[NEt$_4$][Fe(*N*S$_3$)Cl][b]	0.26	0.92
[NEt$_4$][Fe(*N*S$_3$)(CO)][b]	0.22	0.99
[NEt$_4$][Fe(*N*S$_3$)(NO)][c]	0.37	0.68
[{Fe(*N*S$_3$)(CO)$_2$-*S*,*S*′}NiCl(dppe)] **1**	0.07	0.56
[{Fe(*N*S$_3$)(CO)-*S*,*S*′}NiCl(dppe)] **2**	0.23	0.40
[{Fe(*N*S$_3$)(NO)-*S*,*S*′}NiCl(dppe)] **3**	0.40	1.26
[{Fe(*N*S$_3$)(NO)-*S*,*S*′}Ni(CH$_3$)(dppe)] **4**	0.40	1.19
[Ni{Fe(*N*S$_3$)(CO)-*S*,*S*′}$_2$] **5**	0.19	1.40
[Co{Fe(*N*S$_3$)(CO)-*S*,*S*′}$_2$]	0.21	1.29
[Fe{Fe(*N*S$_3$)(CO)-*S*,*S*′}$_2$][b d]	0.21	1.18
	0.62	1.93

[a] i.s. = isomer shift, q.s. = quadrupole splitting ± ≤ 0.01 mm s^{-1}, referenced to iron at 298 K. [b] Ref. 8. [c] Ref. 9. [d] Relative intensity 2 : 1.

Prior to the crystal structure of CODH, we had proposed[12] that trinuclear **5** was a first generation synthetic analogue of the active site of CODH. However, the crystal structure has now revealed a unique {NiFe$_4$S$_5$} assembly at the active site. Complexes **1**–**5** have some features related to the structure of this assembly and that proposed, in the absence of a crystal structure, for the active centre of ACS, in that they possess nickel and iron atoms connected through bridging-sulfur. Trinuclear **5** is a rare example of a complex in which nickel(II) is coordinated in an almost regular tetrahedral geometry by thiolate-sulfur; nickel(II) in a thiolate environment virtually always has a square planar geometry, as the d^8 configuration prefers such a geometry in the presence of strong field donor ligands.

Experimental

General

All manipulations were performed under a dinitrogen atmosphere, unless otherwise stated, using either Schlenk or vacuum line techniques. Solvents were dried over appropriate drying agents and distilled under dinitrogen prior to use. [NiCl$_2$(dppe)$_2$],[27] [NiCl(CH$_3$)(dppe)],[28] [NEt$_4$][Fe(*N*S$_3$)(CO)][9] and [NEt$_4$][Fe(*N*S$_3$)(NO)][10] were prepared by published procedures; all other chemicals were purchased from Aldrich Chemical Co. and used as supplied. Isotopically enriched carbon-^{13}C monoxide (99% atom ^{13}C; 15% atom ^{18}O) was employed in the synthesis of ^{13}C-labelled complexes. IR and UV-vis spectra were recorded on Shimadzu FTIR-8000 and UV-2101PC spectrophotometers, respectively. ^{1}H, ^{31}P and ^{14}N NMR were obtained on a Jeol Lambda 400 spectrometer. Mössbauer spectra were recorded on an ES-Technology MS-105 spectrometer with a 925 MBq ^{57}Co source in a rhodium matrix at ambient temperature. Spectra were referenced to a 25 µm iron foil at 298 K. The X-ray absorption spectra were recorded on SSRL beamline 7–3 with a Si(220) monochromator. Elemental analyses were by Mr A. W. Saunders at the University of East Anglia (CHN), or by Southern Science, Falmer Laboratories, East Sussex (metals).

Preparations

[{Fe(*N*S$_3$)(CO)$_2$-*S*,*S*′}NiCl(dppe)], 1. Under an atmosphere of carbon monoxide, to a stirred suspension of [NiCl$_2$(dppe)] (0.79 g, 1.5 mmol) in MeCN (100 cm^3) was added a solution of [NEt$_4$][Fe(*N*S$_3$)(CO)] (0.61 g, 1.5 mmol) in MeCN (20 cm^3). After 30 min dissolution was complete. On standing overnight a dark brown, crystalline product was obtained, which was collected by filtration, washed with diethyl ether and dried (0.99 g, 83%) (Found: C, 50.8; H, 4.3; N, 2.2; Fe, 6.2; Ni, 7.5. C$_{34}$H$_{36}$ClFeNNiO$_2$P$_2$S$_3$ requires: C, 51.1; H, 4.5; N, 1.8; Fe, 7.0; Ni, 7.4%); λ_{max}/nm (CH$_2$Cl$_2$) 325 (ε/dm^3 mol^{-1} cm^{-1} 18831), 494 (2614); ν_{max}/cm^{-1} (CO) 1944, 2000 (KBr).

Table 7 Crystal and structure refinement data for complexes **1**, **3** and **5**

Structural formula, complex	[{Fe(NS$_3$)(CO)$_2$}-NiCl(dppe)], **1**	[{Fe(NS$_3$)(NO)}NiCl(dppe)]·MeCN, **3**·MeCN	[Ni{Fe(NS$_3$)(CO)}$_2$], **5**
Elemental formula	$C_{34}H_{36}ClFeNNiO_2P_2S_3$	$C_{32}H_{36}ClFeN_2NiOP_2S_3{\cdot}C_2H_3N$	$C_{14}H_{24}Fe_2N_2NiO_2S_6$
Formula weight	798.8	813.8	615.1
Crystal system	Triclinic	Monoclinic	Tetragonal
Space group (no.)	$P\bar{1}$ (no. 2)	$P2_1/c$ (no. 14)	$I4_1cd$ (no. 110)
a/Å	11.5630(11)	11.986(2)	13.5088(4)
b/Å	12.068(2)	19.719(3)	13.5088(4)
c/Å	12.348(2)	15.709(2)	24.371(2)
α/°	91.563(13)	90	90
β/°	91.289(10)	103.345(10)	90
γ/°	92.839(10)	90	90
V/Å^3	1719.9(4)	3612.6(8)	4447.5(4)
Z	2	4	8
μ/mm$^{-1\,a}$	1.36	1.29	2.70
Total no. of reflections measured (not including absences)	5687	8511	1864
R_{int} for equivalent	0.061	0.014	0.013
Total no. of unique reflections	4782	7866	1691
No. of 'observed' reflections ($I > 2\sigma_I$)	2254	5425	1350
Final R indices ('observed' data)	$R1 = 0.058$, $wR2 = 0.112$	$R1 = 0.035$, $wR2 = 0.071$	$R1 = 0.056$, $wR2 = 0.127$
Final R indices (all data)	$R1 = 0.130$, $wR2 = 0.151$	$R1 = 0.060$, $wR2 = 0.084$	$R1 = 0.067$, $wR2 = 0.137$

[a] With Mo-Kα radiation, $\lambda = 0.71069$ Å.

[{Fe(NS$_3$)(CO)-S,S'}NiCl(dppe)], 2. A similar procedure was used to that for the preparation of **1** except the reaction was performed under an atmosphere of dinitrogen or argon. The material could not be obtained analytically pure. ν_{max}/cm^{-1} (CO) 1903 (KBr).

[{Fe(NS$_3$)(NO)-S,S'}NiCl(dppe)]·MeCN, 3·MeCN. To a stirred suspension of [NiCl$_2$(dppe)] (0.34g, 0.64 mmol) in MeCN (50 cm^3) was added, as a layer, [NEt$_4$][Fe(NS$_3$)(NO)] (0.27g, 0.66 mmol) in MeCN (30 cm^3). The reaction mixture was not stirred further. Upon standing overnight a dark brown crystalline material formed that was collected by filtration and dried (0.46g, 88%) (Found: C, 50.2; H, 4.9; N, 5.3; Fe, 6.5; Ni, 7.7. $C_{34}H_{39}ClFeN_3NiOP_2S_3$ requires: C, 50.2; H, 4.8; N, 5.2; Fe, 6.9; Ni, 7.2%); λ_{max}/nm (dmf) 218 (ε/dm^3 mol^{-1} cm^{-1} 20603), 266 (15291); ν_{max}/cm^{-1} (NO) 1667 (KBr); δ_P(162 MHz; solvent dmf; standard P(OMe)$_3$) −113; δ_N (29 MHz; solvent dmf; standard CH_3NO_2) −274.

[{Fe(NS$_3$)(NO)-S,S'}Ni(CH$_3$)(dppe)] 4. To a stirred suspension of [NiCl(CH$_3$)(dppe)] (0.27g, 0.53 mmol) in MeCN (60 cm^3) was added a solution of [NEt$_4$][Fe(NS$_3$)(NO)] (0.24g, 0.59 mmol) in MeCN (10 cm^3). The reaction mixture was stirred for 90 min. Upon standing overnight a brown solid appeared that was collected by filtration, washed with diethyl ether and dried (0.16g, 40%) (Found: C, 52.2; H, 5.2; N, 4.5; Fe, 6.9; Ni, 7.7. $C_{33}H_{39}FeN_2NiOP_2S_3$ requires: C, 52.7; H, 5.2; N, 3.7; Fe, 7.4, Ni, 7.8%); λ_{max}/nm (dmf) 265 (ε/dm^3 mol^{-1} cm^{-1} 30053), 318 (9309), 375 (5053), 464 (2394); ν_{max}/cm^{-1} (NO) 1666 (KBr); δ_H(Me) (400 MHz; solvent dmf; standard SiMe$_4$) 1.3; δ_P(162 MHz; solvent dmf; standard P(OMe)$_3$) −112.

[Ni{Fe(NS$_3$)(CO)-S,S'}$_2$] 5. NiCl$_2$ (0.14 g, 1.08 mmol) was refluxed in anhydrous dmso (18 cm^3) for 1 h. The solution became blue upon refluxing and cooled to a green colour. On to the surface of the cooled solution was layered [NEt$_4$]-[Fe(NS$_3$)(CO)] (0.88 g, 2.15 mmol) dissolved in anhydrous dmso (32 cm^3). The reaction mixture was left undisturbed for 24 h during which time black crystals formed, these were collected by filtration, washed repeatedly with diethyl ether and dried (0.27 g, 41%) (Found: C, 27.5; H, 4.2; N, 4.6; Fe, 17.6; Ni, 9.8. $C_{14}H_{24}Fe_2N_2NiO_2S_6$ requires: C, 27.3; H, 3.9; N, 4.6; Fe, 18.2, Ni, 9.5%); ν_{max}/cm^{-1} (CO) 1933 (KBr).

Crystal structure analyses

The structure analysis of complex **1** is described here. The other analyses followed similar procedures. Crystal data and experimental results are collated in Table 7.

Crystals of **1** are black, square plates. One, *ca* 0.14 × 0.10 × 0.01 mm, was mounted on a glass fibre and coated with epoxy resin. After preliminary photographic examination, this was transferred to a Nonius CAD4 diffractometer (with monochromated radiation) for determination at room temperature of accurate cell parameters (from the settings of 24 reflections, θ = 8–10°, each centred in four orientations) and for measurement of diffraction intensities (5382 unique data were measured to θ = 24° but diffraction was generally weak and, in the refinement process, only the 4782 unique reflections to θ_{max} = 23° were used; of these, 2254 were 'observed' with $I > 2\sigma_I$).

During processing, corrections were applied for Lorentz-polarisation effects, absorption (by semi-empirical ψ-scan methods) and to eliminate negative net intensities (by Bayesian statistical methods). A small deterioration correction was also made. The structure was determined by the direct methods routines in the SHELXS program[29] and refined by full-matrix least-squares, on F^2 in SHELXL.[30] The non-hydrogen atoms were refined with anisotropic thermal parameters. Hydrogen atoms were included in idealised positions; their U_{iso} values were refined freely. At the conclusion of the refinement, $wR_2 = 0.151$ and $R_1 = 0.130$[30] for all 4782 reflections weighted $w = [\sigma^2(F_o^2) + (0.049P)^2]^{-1}$ with $P = (F_o^2 + 2F_c^2)/3$; for the 'observed' data only, $R_1 = 0.058$.

In the final difference map, the highest peaks (to *ca.* 0.47 e Å^{-3}) were close to the Ni atom. Scattering factors for neutral atoms were taken from ref. 31. Computer programs used in this analysis have been noted above or in Table 4 of ref. 32, and were run on a DEC-AlphaStation 200 4/100 in the Department of Biological Chemistry, John Innes Centre.

CCDC reference numbers 135401 (see ref. 11), 156275 (see ref. 12) and 181375.

See http://www.rsc.org/suppdata/dt/b2/b201578c/ for crystallographic data in CIF or other electronic format.

Acknowledgements

The Biotechnology and Biological Sciences Research Council is thanked for funding and the John Innes Foundation for a studentship (to S. L.). S. P. C. acknowledges support from

DOE OBER and NIH GM44380. Drs J. R. Sanders and S. A. Fairhurst of the Department of Biological Chemistry, John Innes Centre are thanked for the supply of NS_3H_3 and EPR spectroscopy, respectively.

References

1 A. Volbeda, M.-H. Charon, C. Piras, E. C. Hatchikian, M. Frey and J. C. Fontecilla-Camps, *Nature (London)*, 1995, **373**, 580.

2 A. Volbeda, E. Garcin, C. Piras, A. L. de Lacey, V. M. Fernandez, E. C. Hatchikian, M. Frey and J. C. Fontecilla-Camps, *J. Am. Chem. Soc.*, 1996, **118**, 12989.

3 S. Niu, L. M. Thomson and M. B. Hall, *J. Am. Chem. Soc.*, 1999, **121**, 4000; L. De Gioia, P. Fantucci, B. Guigliarelli and P. Bertrand, *Inorg. Chem.*, 1999, **38**, 2658; P. Amara, A. Volbeda, J. C. Fontecilla-Camps and M. J. Field, *J. Am. Chem. Soc.*, 1999, **121**, 4468.

4 R. P. Happe, W. Roseboom, A. Pierik, S. P. J. Albracht and K. A. Bagley, *Nature (London)*, 1997, **385**, 126.

5 H. Dobbek, V. Svetlitchnyi, L. Gremer, R. Huber and O. Meyer, *Science*, 2001, **293**, 1281.

6 C. L. Drennan, J. Heo, M. D. Sintchak, E. Schreiter and P. W. Ludden, *Proc. Natl. Acad. Sci. U.S.A.*, 2001, **98**, 11973.

7 C. R. Staples, J. Heo, N. J. Spangler, R. L. Kerby, G. P. Roberts and P. W. Ludden, *J. Am. Chem. Soc.*, 1999, **121**, 11034; J. Heo, C. R. Staples, C. M. Halbleib and P. W. Ludden, *Biochemistry*, 2000, **39**, 7956.

8 J. C. Fontecilla-Camps and S. W. Ragsdale, *Adv. Inorg. Chem.*, 1999, **47**, 283.

9 S. C. Davies, D. L. Hughes, M. C. Durrant, R. L. Richards and J. R. Sanders, *J. Chem. Soc., Dalton Trans.*, 2000, 4694.

10 S. C. Davies, D. J. Evans, D. L. Hughes, M. Konkol, R. L. Richards, J. R. Sanders and P. Sobota, *J. Chem. Soc., Dalton Trans.*, 2002, 2473.

11 S. C. Davies, D. J. Evans, D. L. Hughes, S. Longhurst and J. R. Sanders, *Chem. Commun.*, 1999, 1935.

12 M. C. Smith, S. Longhurst, J. E. Barclay, S. P. Cramer, S. C. Davies, D. L. Hughes, W.-W. Gu and D. J. Evans, *J. Chem. Soc., Dalton Trans.*, 2001, 1387.

13 D. J. Evans, *J. Chem. Res. (S)*, 2001, 297.

14 S. C. Davies, D. L. Hughes, Z. Janas, L. Jerzykiewicz, R. L. Richards, J. R. Sanders and P. Sobota, *Chem. Commun.*, 1997, 2699.

15 C.-H. Lai, J. H. Reibenspies and M. Y. Darensbourg, *Angew. Chem., Int. Ed. Engl.*, 1996, **35**, 2390.

16 F. Osterloh, W. Saak, D. Haase and S. Pohl, *Chem. Commun.*, 1997, 979.

17 F. Osterloh, W. Saak, D. Haase and S. Pohl, *Chem. Commun.*, 1996, 777.

18 G. J. Colpas, R. O. Day and M. J. Maroney, *Inorg. Chem.*, 1992, **31**, 5053.

19 D. K. Mills, Y. M. Hsiao, P. J. Farmer, E. V. Atnip, J. H. Reibenspies and M. Y. Darensbourg, *J. Am. Chem. Soc.*, 1991, **113**, 421.

20 S. Li and M. B. Hall, *Inorg. Chem.*, 2001, **40**, 18.

21 G. Davidson, S. B. Choudhury, Z. Gu, K. Bose, W. Roseboom, S. P. J. Albracht and M. J. Maroney, *Biochemistry*, 2000, **39**, 7468.

22 S. G. Rosenfield, W. H. Armstrong and P. K. Mascharak, *Inorg. Chem.*, 1986, **25**, 3014.

23 A. Müller and G. Henkel, *Z. Naturforsch. Teil B*, 1995, **50**, 1464.

24 T. C. Higgs, D. Ji, R. S. Czernuszewicz, K. Spartalian, C. J. O'Connor, C. Seip and C. J. Carrano, *J. Chem. Soc., Dalton Trans.*, 1999, 807.

25 J. H. Enemark and R. D. Feltham, *Coord. Chem. Rev.*, 1974, **13**, 339.

26 C. A. Brown, M. A. Pavlosky, T. E. Westre, Y. Zhang, B. Hedman, K. O. Hodgson and E. I. Solomon, *J. Am. Chem. Soc.*, 1995, **117**, 715; C. Hauser, T. Glaser, E. Bill, T. Weyhermüller and K. Wieghardt, *J. Am. Chem. Soc.*, 2000, **122**, 4352 and references therein.

27 S. C. Davies, R. A. Henderson, D. L. Hughes and K. E. Oglieve, *J. Chem. Soc., Dalton Trans.*, 1998, 425.

28 T. Yamamoto, T. Kohara, K. Osakada and A. Yamamoto, *Bull. Chem. Soc. Jpn.*, 1983, **56**, 2147.

29 G. M. Sheldrick, *Acta Crystallogr. Sect. A*, 1990, **46**, 467.

30 G. M. Sheldrick, SHELXL, Program for crystal structure refinement, University of Göttingen, Germany, 1993.

31 *International Tables for X-ray Crystallography*, Kluwer Academic Publishers, Dordrecht, 1992, vol. C, pp. 500, 219 and 193.

32 S. N. Anderson, R. L. Richards and D. L. Hughes, *J. Chem. Soc., Dalton Trans.*, 1986, 245.